Canadian Chemical Transactions

ISSN 2291-6458 (Print), ISSN 2291-6466 (Online)
Year 2013 | Volume 1 | Issue 4 | Page 238-252

Research Article

DOI:10.13179/canchemtrans.2013.01.04.0035

Au(III)-Surfactant Complex-Assisted Anisotropic Growth of Advanced Platonic Au-Nanoparticles

Shaeel Ahmed AL-Thabaiti[1], Javed Ijaz Hussain[2], Athar Adil Hashmi[2], and Zaheer Khan[2]*

[1]Department of Chemistry, Faculty of Science, King Abdulaziz University, P.O. Box 80203, Jeddah-21413, Saudi Arabia
[2]Nanoscience Research Laboratory, Department of Chemistry, Jamia Millia Islamia (Central University), New Delhi-110025, India

*Corresponding Author, *Email:* drkhanchem@yahoo.co.in

Received: *August 29, 2013* ***Revised:*** *September 30, 2013* ***Accepted:*** *October 7, 2013* ***Published:*** *October 8, 2013*

Abstract: Growth of Au-nanoparticles (hexahedral, irregular shaped, polyhedral and pentagons, triangular shaped) is investigated using oxalic acid in the presence of aqueous solution of cetyltrimethylammonium bromide (CTAB) and sodiumdodecyl sulphate (SDS) for the first time. Interestingly, upon addition of tetrachloroauric(III) ($HAuCl_4$) to a solution of CTAB, a perfect transparent yellowish-orange colored appears very fast, where as such type of color did not formed with SDS. Intensity of the resulting orange color decreases with [CTAB] and orange precipitate appeared after 24 h. These results are indicative to the formation of $[AuBr_4]^-$ and cetyltrimethylammonium-Au(III) $[CTA^+$-$AuCl_4^-]$ complexes simultaneously. The role of [CTAB], [oxalic acid], [SDS] and $[HAuCl_4]$ in the formation of platonic Au-nanoparticles have been studied using UV-vis absorption and transmission electron microscopy (TEM). The nanoparticles aggregated in a beautiful manner to yield nano-chains and nanonetworks-like gold with dimensions between 10 and 37 nm.

Keywords: Gold nanoparticles, Oxalic acid, Morphology, CTAB, SDS, Kinetics

1. INTRODUCTION

The literature is replete with the investigations of the use of different stabilizers (polymers, surfactants, carbohydrates, proteins, lipids and organic solvents) for carrying out the anisotropic syntheses (penta-twinned, nanorods, needle-like, cubic, and octahedral, stars, etc.) of Ag- , Au- and Ag-Au bimetallic- nanoparticles by a number of weak and strong reductants [1]. Morphology of resulted nanoparticles strongly depends on the experimental conditions, i. e., presence of stabilizers, concentrations of reactants, pH, order of mixing, temperature, and nature of the methods [2]. Cataionic surfactants have been considered as a soft colloidal template in controlling the size and shape of inorganic nano-crystals due to the fact that colloidal templates are highly dynamic in nature and additionally

ISSN 2291-6458 (Print), ISSN 2291-6466 (Online)
Year 2013 | Volume 1 | Issue 4 | Page 238-252

Table 1. Effects of [oxalic acid], [stabilizers] and [$HAuCl_4$] on the rates constants, color and λ_{max} of AuNPs.

10^4 [oxalic acid]	[stabilizers]		10^4[$HAuCl_4$]	10^4k_{obs}	color and λ_{max}
	10^4[CTAB]	10^3[SDS]			
(moldm^{-3})	(mol dm^{-3})	(mol dm^{-3})	(mol dm^{-3})	(s^{-1})	(nm)
0.0	0.0	0.0	3.0	-	pale- yellow;
20.0	0.0	0.0	3.0	-	yellowish-turbid
20.0	0.0	0.0	4.0	-	yellowish turbid
20.0	20.0	0.0	3.0	5.6	orange; 400 & 475
40.0	20.0	0.0	3.0	5.7	yellow; 400 & 475
40.0	20.0	0.0	4.0	6.2	orange yellow; 475
20.0	10.0	0.0	4.0	5.8	orange; 575 & 650
20.0	20.0	0.0	4.0	6.2	orange ; 650
20.0	30.0	0.0	4.0	6.6	orange yellow
20.0	40.0	0.0	4.0	7.0	orange yellow
20.0	0.0	20.0	4.0	4.1	purple; 550
20.0	0.0	30.0	4.0	4.5	purple; 550

provide colloidal stability for the synthesised nanoparticles [3]. Esumi et al. reported an irradiation method for the preparation of rod-like anisotropic gold colloids in rod-like micellar solution of cationic micelles of hexadecyltrimethylammonium chloride surfactant, which operates as a soft template [4]. Nikoobakht and El- Sayed reported a seed-growth method to the preparation of single crystalline Au nanorods in high yields using CTAB-capped Au seeds for the first time [5]. Sau and Murphy [6] showed that platonic AuNPs (hexahedra cubes ; four squares and octahedra ; four triangles) have been obtained in different yield at low [CTAB] , high [ascorbic acid] and high [CTAB] , low [ascorbic acid], respectively, and suggested that low [CTAB] favors faster deposition of Au^0 atoms onto the {111} facets of the seeds, until they disappear, giving rise to {100} facets exclusively. Chen and his coworkers [7] used of Ag triangular platelets as seeds for the synthesis of branched AuNPs (monopods, bipods, tripods and tetrapods) by reduction of gold ions with ascorbic acid in alkaline CTAB solution.

In general, citrate- and CTAB-capped nanoparticles used for the isotropic growth of AuNPs in presence of ascorbic acid and it has been accepted that CTAB has turned out to be very effective in the shape-controlled synthesis of Au-nanorods (the average aspect ratio of the Au-nanorods increased and the nanorod growth rate decreased as the cationic surfactant headgroup became larger) [6, 8]. Anionic, nonionic and zwitter ionic surfactants were also used for the synthesis of gold nanostructures under the same experimental conditions, leading to the formation of multiple anisotropic nanostructures (rugged, leaf-like, dendritic, and tadpole-shaped with well-defined and dispersed morphology) [9]. Xia et al. [10] and Qi and co-workers [11] reported a facile method for preparing ultrathin Au-nanowires and porous Au-nanobelts using [(oleylamine)AuCl] complex chains formed through aurophilic attraction and metal–surfactant complex precursor nanobelts formed by $HAuCl_4$ and a bola-form surfactant containing two quaternary ammonium head groups, respectively. Xiao and Qi in their pioneering feature article

ISSN 2291-6458 (Print), ISSN 2291-6466 (Online)
Year 2013 | Volume 1 | Issue 4 | Page 238-252

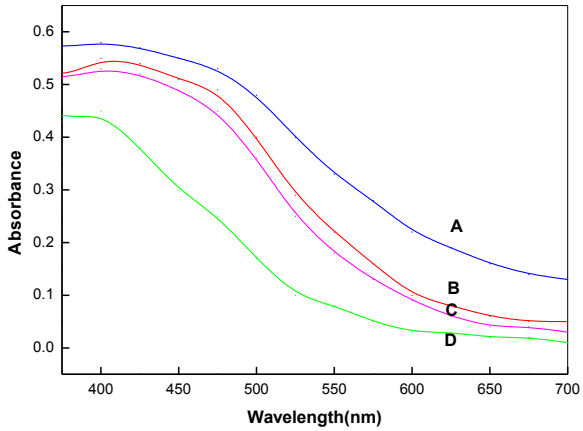

Fig. 1. Plots showing the formation of Au(III)-CTAB complex. *Reaction conditions*: [$HAuCl_4$] = 20.0 × 10^{-4} mol dm^{-3}; [CTAB] = 10.0 (A), 20.0 (B), 40.0 (C) and 50.0 × 10^{-4} mol dm^{-3} (D).

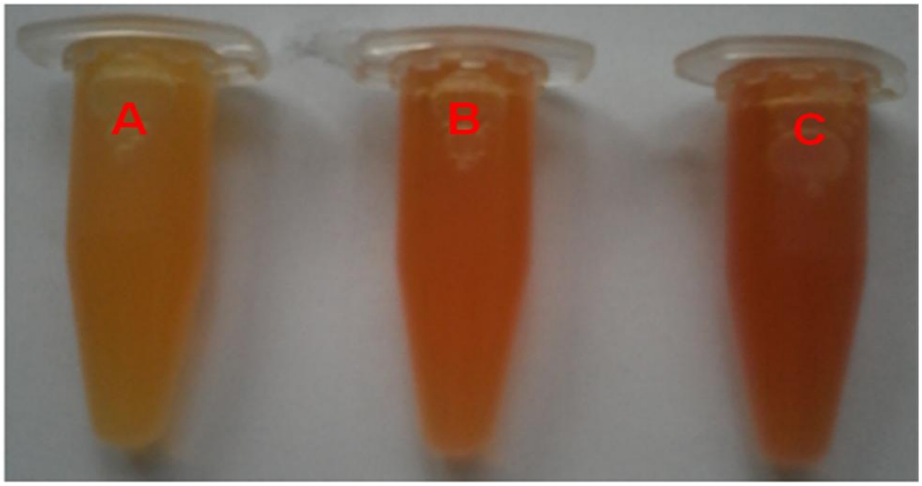

Fig. 2. Optical images of Au(III)-CTAB complex. *Reaction conditions*: [$HAuCl_4$] = 4.0 × 10^{-4} mol dm^{-3}; [CTAB] = 20.0 (A), 40.0 (B), and 60.0 × 10^{-4} mol dm^{-3} (C).

highlighted the some recent progress in the synthesis of gold nanocrystal assisted by single surfactants, mixed surfactants, supramolecular surfactants, as well as metal–surfactant complex templates [1e]. These workers also pointed out that surfactants can act as efficient adsorbates or capping agents, significantly affect the formation of crystal seeds, form ordered structures through either self-assembly in solution or co-assembly with inorganic species, and strongly interact with the reacting species and the growing nanocrystals.

Turkevitch and his coworkers 1951, reported a simple chemical reduction method for the synthesis of AuNPs (ca. 20 nm) using gold(III) derivatives and citric acid in water [12]. Due to an effective capping agent capable of blocking surfaces from chemical reactivity, use of citric acid or its sodium salt has been the subject of various investigators for the synthesis of Au- and Ag-NPs [13]. Silver nanoplates with an extremely high aspect ratio (up to over 400) have been successfully synthesized by combining the concepts of selective ligand adhesion and seeded growth methods. Citrate ligands are used

ISSN 2291-6458 (Print), ISSN 2291-6466 (Online)
Year 2013 | Volume 1 | Issue 4 | Page 238-252

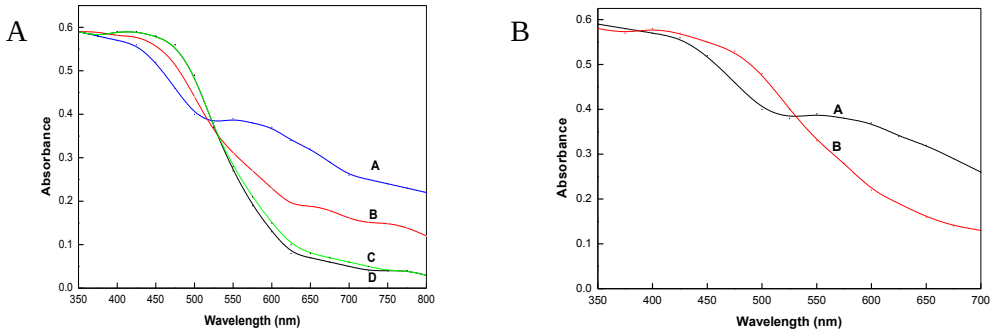

Fig. 3. A- Effect of [CTAB] on the anisotropic growth of gold-nanocrystals. *Reaction conditions*: [$HAuCl_4$] = 4.0 × 10^{-4} mol dm^{-3}; [oxalic acid] = 20.0 ×10^{-4} mol dm^{-3}; [CTAB] = 10.0 (A), 20.0 (B), 30.0 (C) and 40.0 ×10^{-4} mol dm^{-3} (D). B-Comparison between the SPR band positions of AuNPs (A) and Au(III)-CTAB complex (B).

as the sole surfactant to effectively block overgrowth on the basal {111} facets and only allow growth in the lateral direction [14]. Yin et al. [15] carried out the systematic studies to the synthesis of silver nanoplates by the direct chemical reduction route using citric acid, hydrogen peroxide and sodium borohydride. These investigators also identified the specific roles of each reagent and determined that the list of ligends' with selective adhesion to Ag (111) facets can be expanded from citrate, which has been previously regarded as a "magic" irreplaceable ligand, to many di- and tricarboxylate compounds whose two nearest carboxylate groups are separated with two or three carbon atoms. Recently, we have reported the Au(III)-CTAB complex reduction by ascorbic acid [16]. However, the use of oxalic acid (di-carboxylic acid, sacrificial electron donors and its oxidation product, i.e., CO_2, has no complex-forming tendency) in the surface chemistry of Au-NPs is not yet well-known. To the best of our knowledge, there are no reports about the use of oxalic acid-Au(III) redox reaction in the surfactant-induced anisotropic growth of AuNPs. Our goal in this study was to (i) investigate the Au(III) interactions with cationic and anionic surfactants. For this purpose we had chosen CTAB and SDS and (ii) to prepare the AuNPs using oxalic acid as reducing-agent. The observed results and the probable explanations detailed in this paper. The present strategy for generating Au-nanoparticles could be extended to the synthesis of other noble metal particles using other surfactants bearing different polar head groups. This paper will also be an ignited clue for CTAB and SDS applications in engineering nanometer-sized devices and would be useful for the shape-controlled synthesis of metal nanoparticles for desired functional properties.

2. Experimental Methods

2.1. Chemicals

Deionized water was used as solvent to prepare all of the aqueous solutions. Oxalic acid ($C_2H_2O_4.2H_2O$, reductant, 99%), chloroauric acid ($HAuCl_4$, molecular weight 393.79 gmol), cetyltrimethylammonium bromide and sodiumdodecyl sulphate were obtained from Merck India and used with out further purification. All the glass wares were washed with aqua regia solution (HCl / HNO_3, 3:1), then rinsed thoroughly with deionized and CO_2 free water before use.

2.2. Instruments

The spectrophotometric analysis of the solutions was carried out using Perkin Elmer (Lambda 25) UV-Vis spectrophotometer. Morphological details of the synthesized AuNPs were studied using

ISSN 2291-6458 (Print), ISSN 2291-6466 (Online)
Year 2013 | Volume 1 | Issue 4 | Page 238-252

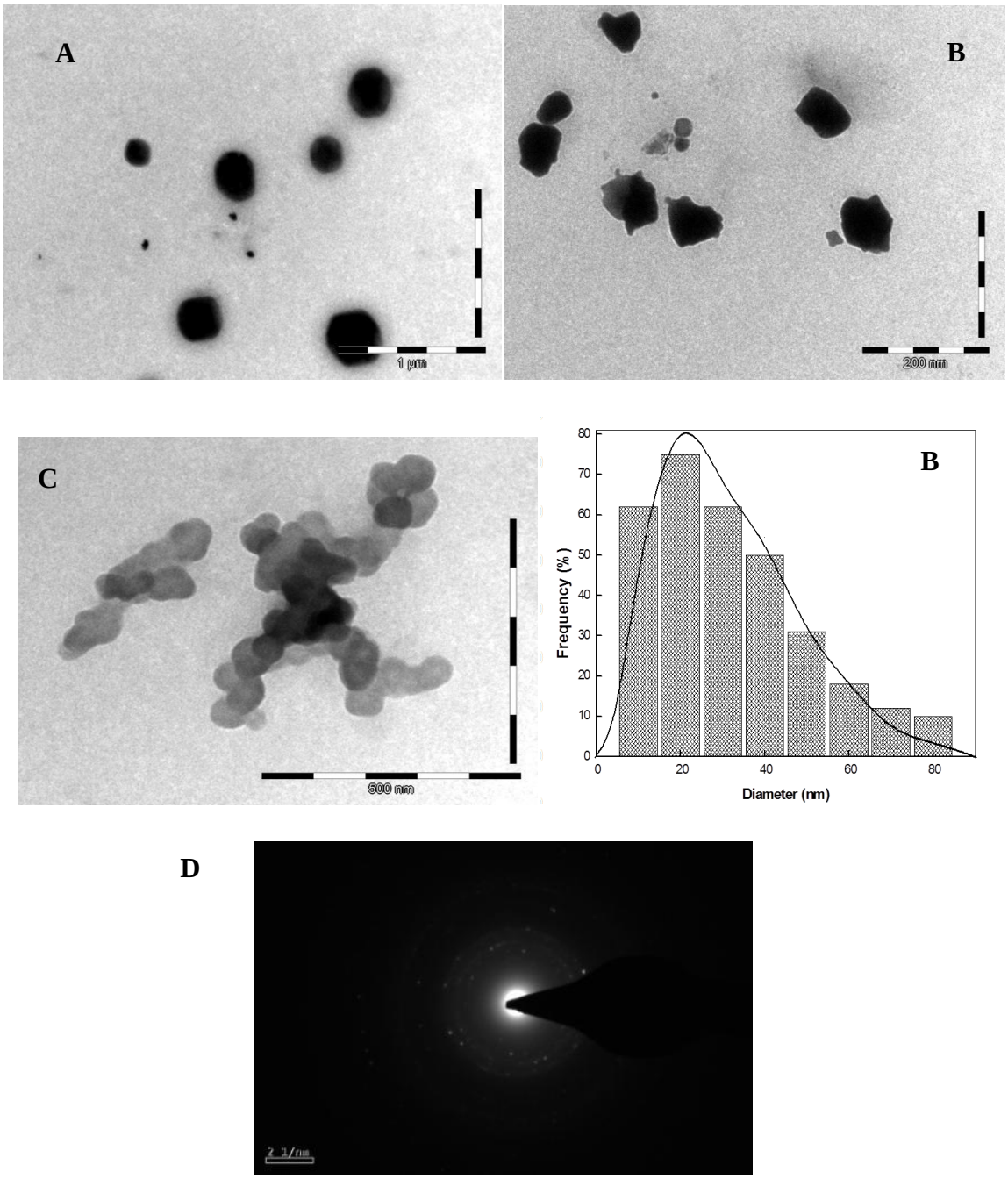

Fig.4. TEM images (A, B, C), size distribution (B) and selected electron diffraction patterns of gold-nanocrystals (D) in presence of [CTAB] = 20.0 $\times 10^{-4}$ mol dm^{-3}. *Reaction conditions*: [$HAuCl_4$] = 4.0 $\times$ 10^{-4} mol dm^{-3}; [oxalic acid] = 20.0 (A) and 40.0 $\times$ 10^{-4} mol dm^{-3} (B).

transmission electron microscopy (JEOL, JEM-1011; Japan). Samples were prepared by placing a drop of working solution on a carbon-coated standard copper grid (300 mesh) operating at 80 kV. An Accumet, Fisher Scientific digital pH meter 910 fitted with a combination electrode was used for pH measurements.

2.3. Kinetic method

The required solution of $HAuCl_4$, CTAB and H_2O for dilution (except oxalic acid) was taken in a

ISSN 2291-6458 (Print), ISSN 2291-6466 (Online)
Year 2013 | Volume 1 | Issue 4 | Page 238-252

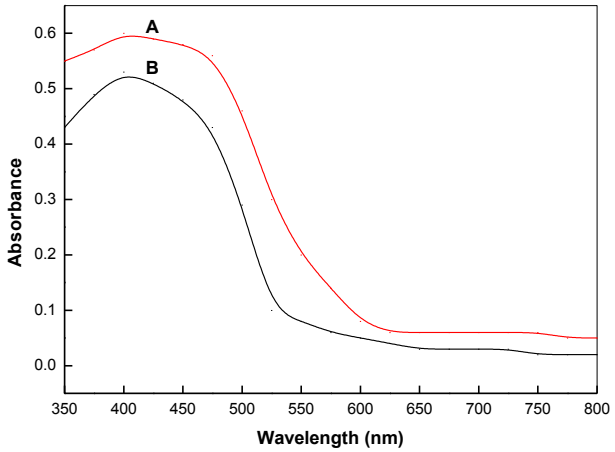

Fig. 5. Effects of [$HAuCl_4$] on the SPR band of gold-nanocrystals. *Reaction conditions:* [CTAB] = 20.0 × 10^{-4} mol dm^{-3}; [oxalic acid] = 40.0 ×10^{-4} mol dm^{-3} ; [$HAuCl_4$] = 3.0 (A) and 4.0 × 10^{-4} mol dm^{-3} (B).

two-necked reaction vessel equipped with a double-surface condenser to check evaporation. The reaction was initiated with the addition of required volume of thermally equilibrated oxalic acid solution. The zero time was taken when half of the oxalic acid solution has been added. The progress of the reaction was followed spectrophotometrically at 425 nm with a spectronic-21D u.v.-vis spectrophotometer Quartz cuvettes of path length 1 cm were used. Apparent first-order rate constants were calculated from the initial part of the slopes of the plots of ln (a / (1 – a)) versus time, where a = At / Aα (absorbance At at time t and Aα is the final absorbance) with a fixed time method [17]. In the present study, it is necessary to point out that the plots of ln(a / (1 – a)) versus time are deviates from the linearity. Duplicate runs gave results that were reproducible to within ± 4 %. Other details of kinetic procedure were the same as described elsewhere [18, 19]. The pH of the reaction mixture was also measured at the end of each kinetic experiment and observed that pH drift during the course of the reaction is very small (with in 0.04 unit).

2.4. Identification of reaction products and intervention of free radicals

For the oxidation product of oxalic acid, qualitative analysis of oxidized reaction mixture was performed. CO_2 was quantitatively detected by bubbling N_2 gas through the reaction mixture and passing the liberated gas through a tube containing $Ba(OH)_2$ solution and then estimated by titration with standard HCl solution [20]. Test for free radicals (Polymerization study) involvement in the reaction was examined by the polymerization of initially added acrylonitrile scavenger in the reaction mixture ($HAuCl_4$ = 3.0 × 10^{-4} mol dm^{-3}, [oxalic acid] = 20.0 × 10^{-4} mol dm^{-3} and [CTAB] = 20.0 × 10^{-4} mol dm^{-3}). Appearance of white precipitate after some time indicates the free radical intervention during the oxidation of oxalic acid.

2.5. Preparation of gold nanoparticles

It has been established that the choice of the best conditions for the synthesis of prefect transparent colored sols of gold is a critical problem that we address first. In the first set of experiments, a required amounts of oxalic acid was added to a solutions containing required concentrations of $HAuCl_4$ and CTAB at 30 ^oC. It was observed that yellow colored reaction mixture became orange after the addition of oxalic acid. In the second set of experiments, $HAuCl_4$ solutions were added to a solution containing ascorbic acid and CTAB . At higher [$HAuCl_4$] (≥ 6.0 × 10^{-4} mol dm^{-3}), the reaction mixtures

ISSN 2291-6458 (Print), ISSN 2291-6466 (Online)
Year 2013 | Volume 1 | Issue 4 | Page 238-252

becomes turbid and a yellowish precipitate was appeared instead of prefect transparent gold sols. The best experimental conditions to the preparation of gold nanoparticles are the oxalic] $\geq 10.0 \times 10^{-4}$ mol dm^{-3} , $HAuCl_4 < 3.0 \times 10^{-4}$ mol dm^{-3}), and CTAB ($\geq 10.0 \times 10^{-4}$ mol dm^{-3}.

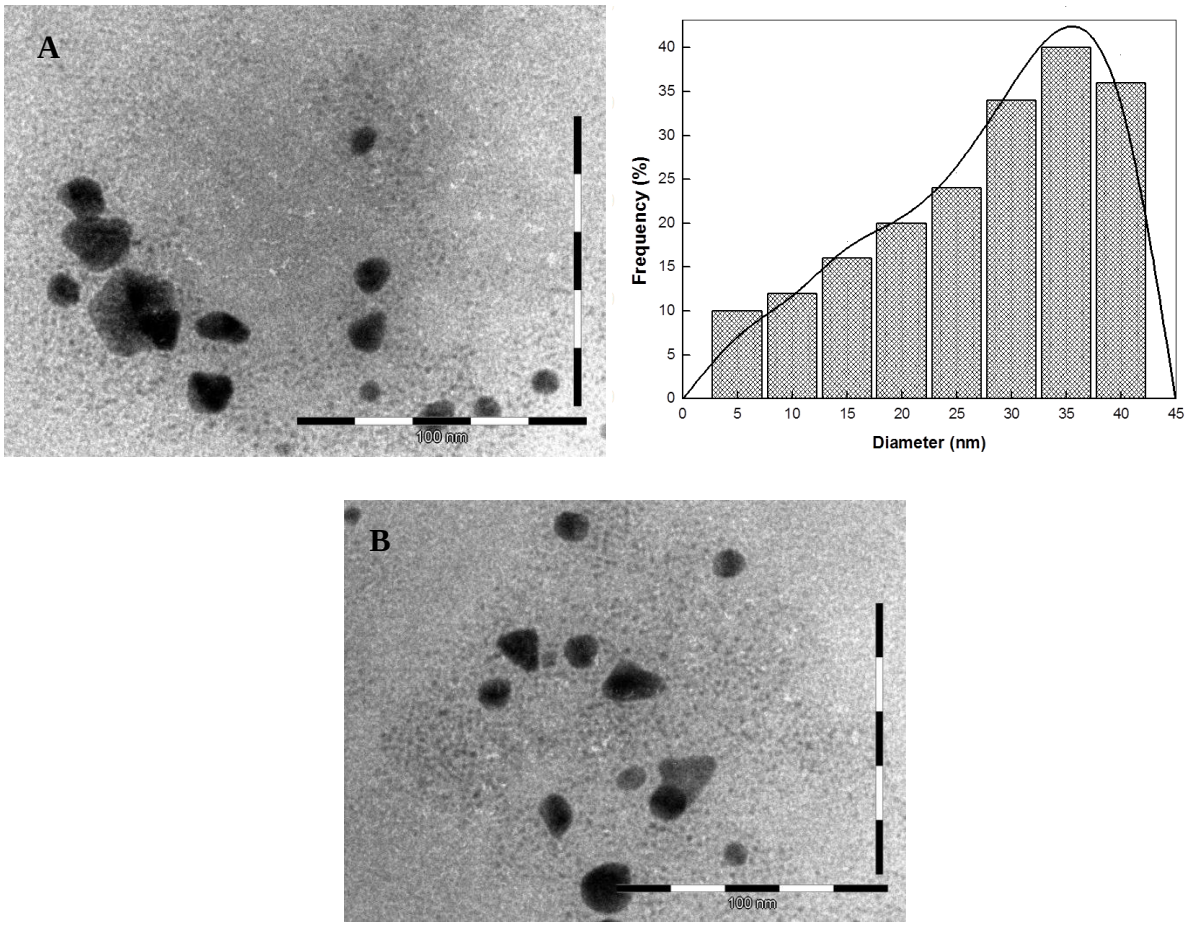

Fig. 6. TEM images and size distribution gold-nanocrystals in presence of [SDS] = 20.0×10^{-4} mol dm^{-3}. *Reaction conditions*: [$HAuCl_4$] = 4.0×10^{-4} mol dm^{-3}; [oxalic acid] = 20.0×10^{-4} mol dm^{-3} .

3. RESULTS AND DISCUSSION

3.1. Au(III) interactions with CTAB and SDS

In a typical experiment, $HAuCl_4$ solution of (20.0×10^{-4} mol dm^{-3}) was taken in a Erlenmeyer flask, and then different CTAB concentrations (from 10.0×10^{-4} to 50.0×10^{-4} mol dm^{-3}) were added . Visual observation showed that the color of the reaction mixture ($HAuCl_4$ + CTAB) changed from pale yellow, orange, to brown with within the 5 min. The appearance of brown color was due to the ligand to metal charge transfer and it provides a convenient spectroscopic signature to indicate the formation of Au(III)-CTAB ion-pair complex [21]. The spectra of color were monitored by measuring the absorbance of the solution at different concentrations of CTAB in a wavelength ranging from 300 to 700 nm. Fig. 1 shows that the absorbance of the yellowish-orange color decreases with increasing CTAB concentration. It is important to recall that each spectrum showed one broad covering the whole visible region of the spectrum with a broad shoulder at 450 nm. The negative effect of the CTAB is probably due to their

ISSN 2291-6458 (Print), ISSN 2291-6466 (Online)
Year 2013 | Volume 1 | Issue 4 | Page 238-252

interaction with the bromide counter-ion of the surfactant monomers, Optical images of $HAuCl_4$ + CTAB aqueous solutions are also shown in Fig. 2, indicating that the typical color changed from pale yellow, orange, to brown with increasing CTAB concentrations. Interestingly, the reaction mixture turned turbidorange and a golden yellowish- precipitate appears after some time, the precipitate was filtered, washedwith cold water, dried and infra-red spectra recorded. The mechanism to the formation of complexbetween the $HAuCl_4$ and CTAB through ligand exchange reactions is summarized in Scheme 1.

$$CH_3(CH_2)_{15}(CH_3)_3\overset{+}{N}\overset{-}{Br} \rightleftharpoons CH_3(CH_2)_{15}(CH_3)_3\overset{+}{N} + Br^- \quad (1)$$

$$HAuCl_4 \longrightarrow AuCl_4^- + H^+ \quad (2)$$

$$[AuCl_4]^- + 4Br^- \xrightarrow{Fast} [AuBr_4^-] + 4Cl^- \quad (3)$$

(orange)

Scheme 1. Ligand substitution between CTAB and $HAuCl_4$

In Scheme 1, Eq (1) represents the ionization CTAB molecule (at lower concentrations, surfactants simply behave as an electrolyte). Eq. (2) shows the complete dissociation of $HAuCl_4$ into $AuCl_4^-$ (square planer geometry) and H^+ ions in aqueous solution. Finally, $AuCl_4^-$ converted into $AuBr_4^-$ through a multi-step ligand exchange reactions that occurs in less than a minute [22], which leads to the formation of perfect transparent and stable orange-yellow colored complex. On the other hand, ion-pair complex, $CH_3(CH_2)_{15}(CH_3)_3N$-$AuCl_4$ formation between $AuCl_4^-$ and positive head group of CTAB cannot be ruled out completely (Eq.(4)) [1b, 23].

$$CH_3(CH_2)_{15}(CH_3)_3\overset{+}{N} + AuCl_4^- \xrightarrow{Fast} CH_3(CH_2)_{15}(CH_3)_3N\text{-}AuCl_4 \quad (4)$$

In order to see any type of interaction and/or reactivity of $HAuCl_4$ towards anionic surfactant, experiments were performed under different concentrations of SDS (from 10.0×10^{-3} to 50.0×10^{-3} mol dm^{-3}) at fixed [$HAuCl_4$] (20.0×10^{-4} mol dm^{-3}). Preliminary observations showed that the reaction mixture does not become yellowish-orange in presence of SDS. The observation is not unexpected; the anionic head group ($-OSO_3^-$) of SDS monomers and/or micelles did not form ion-pair with $HAuCl_4^-$ due to the electrostatic repulsion.

3.2. Au(III) reduction by oxalic acid in presence of CTAB

Our synthetic method was one-pot and simple; the AuNPs are prepared by reduction of $HAuCl_4$ with a mild reducing agent (e. g., oxalic acid) in presence of CTAB and/or SDS at room temperature. Oxalic acid readily reduces $HAuCl_4$ to metallic gold, leading to a yellowish-purple precipitate which may be due to the uncontrolled growth of AuNPs. In order to prepare a prefect transparent gold sol, CTAB and SDS were used as a stabilizing-, capping- and structural directing- agents. The results of various experiments are summarized in Table 1. To examine the role of CTAB concentration dependence on $HAuCl_4$ reduction by oxalic acid and AuNPs formation, absorption spectra were recorded after 30 min mixing of the reaction mixture ($HAuCl_4$ + CTAB) with an oxalic acid aqueous solution at different CTAB concentrations (Fig. 3 A and B). The two broad shoulder centered at 400 (for the gold(III) bromide) and 575 nm was observed which originating from the surface plasmon of the AuNPs [24]. As concentration of CTAB increased, the absorption band centered at 575 nm decreased (Fig. 3A) gradually in intensity

ISSN 2291-6458 (Print), ISSN 2291-6466 (Online)
Year 2013 | Volume 1 | Issue 4 | Page 238-252

and remains constant at higher CTAB concentration (≥ 30.0 × 10^{-4} mol dm^{-3}). This decrease coincides with a shift to higher wavelength shoulder centered 400 nm, suggesting that AuNPs were formed following the reduction of $AuBr_4^-$. Fig. 3B clearly indicates that a rapid change in the shape of the CTAB-$HAuCl_4$ spectra upon the addition of oxalic acid was observed for the reaction with a low [oxalic acid]. Specifically, a noticeable absorption feature at around 575 nm appeared in the spectrum, indicating the formation of AuNPs. It can be seen that by increasing the concentrations of CTAB, the longitudinal plasmon band redshifts and its intensity decreases. Size distribution measurements confirm that the aspect ratio of AuNPs increases as shown in Fig.3. These results also suggests that an increase in CTAB concentration facilitates the formation of micelles, more and more $AuBr_4^-$ gets incorporated into the micellar phase. Segregation deactivates the substrate since $AuBr_4^-$ in one micelle cannot react with oxalic acid. The reduction can take place only when both $AuBr_4^-$ and oxalic acid are located inside the same surfactant cavity, which must also contain growing nuclei [25].

The size and shape of AuNPs were examined for different oxalic acid concentrations at fixed $HAuCl_4$ concentration using TEM. Interestingly, a significant amount of small and large with a quite broad size distribution AuNPs was observed under TEM after the addition of oxalic acid for the reaction containing $HAuCl_4$ + CTAB (4.0 ×10^{-4} mol dm^{-3} and 40.0 × 10^{-4} mol dm^{-3}). Surprisingly, a different distinguishable evolution pattern is observed (Fig. 4). For a reaction with a low [oxalic acid], single, poly-dispersed and close to hexahedral particles were the major products, although some small unshaped particles might be observed (Fig. 4A). As the concentrations of oxalic acid increased, hexahedral shape changed to the irregular morphology and tendency of aggregation increased (Fig 4 B and C). The hexagon plate, or other polygon plates are both based on the triangular plate. Subsequently, these small AuNPs evidently started to form aggregates, most of the aggregates being in irregular nano-chains and nanonetworks-like gold. The aggregations of AuNPs due to a plurality of gold nanograins connected with each other by carboxyl groups of oxalic acid, which acting as a reducing- and a stabilizing- and/or shape-directing agent (wherein the carboxylic acid comprises at least two carboxyl groups). These nano-chains aggregates were crystalline and are in good agreement similar to that observed in a few recent reports [26]. It is been established that broadening and red shifts of the plasmon band of AuNPs occur when the metal particles agglomerate to form particle networks [27]. We did not observed the appearance of SPR band at ca. 550 to 600 nm at higher [oxalic acid] (Fig.5). Our results are in good agreement with the observations of Liz-Marzan et al. and to the formation of different shape and size AuNPs which strong depends on the ratio of the reactants [28]. Thus, we may safely conclude that the morphology of the AuNPs changes with the molar ratio of the $HAuCl_4$ to the oxalic acid. Therefore, the method can further include a step of controlling the morphology of the AuNPs by adjusting the molar ratio of the gold ions to the carboxylic acid [26-28].

3.3. Au(III) reduction by oxalic acid in presence of SDS

In order to see the role of SDS during the reduction of $HAuCl_4$ by oxalic acid, a series of experiments were also carried out with two different SDS concentrations (20.0 and 30.0 × 10^{-4} mol dm^{-3}) at fixed oxalic acid concentration (20.0 × 10^{-4} mol dm^{-3}) and $HAuCl_4$ concentration (4.0 × 10^{-4} mol dm^{-3}). The results of these experiments, visual observations, TEM images and spectra are summarized in Table 1, Figs. 6 and 7, respectively. Fig. 6 shows that the AuNPs constitute different irregular, pentahedral, triangular and truncated nano-sheets. A spectrum of AuNPs prepared in SDS has one well defined band at 550 nm, which is the characteristic purple colored Au-sol. We did not observed any peak and/or shoulder in the vicinity of 400 to 500 nm (Fig. 7), reveal that there is no any type of interactions between $HAuCl_4$ and negative head group of SDS micelles. Fig. 7 also shows that concentrations of SDS has no significant

ISSN 2291-6458 (Print), ISSN 2291-6466 (Online)
Year 2013 | Volume 1 | Issue 4 | Page 238-252

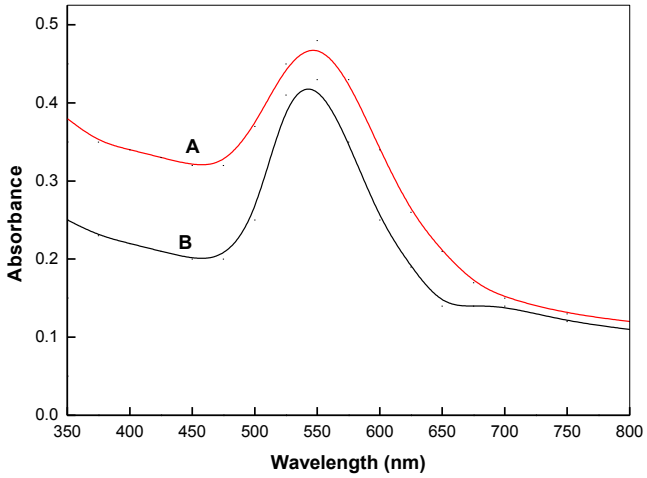

Fig 7. Effects of [SDS] on the on the anisotropic growth of gold-nanocrystals. *Reaction conditions:* [oxalic acid] = 20.0 ×10^{-4} mol dm^{-3}; [$HAuCl_4$] = 4.0 ×10^{-4} mol dm^{-3}; [SDS] = 30.0 (A) and 20.0 × 10^{-4} mol dm^{-3} (B).

effect on the shape, and position of the wavelength maxima, indicating that SDS did not acted as a shape-directing. Taking into account the role of CTAB and SDS surfactants, interestingly, it is to be noted that both surfactants have different behavior in the stabilization and/or capping of AuNPs (from Figs. 1 to 7). This may be attributed to solubilization/ incorporation of the reactants and /or AuNPs into the micellar phase and adsorption of AuNPs on the surface of CTAB and SDS micelles.

To explain the different behavior of CTAB and SDS micelles, the presence of negative charge on $AuCl_4^-$ and its metal particles must be considered. It is certainly possible that the $AuCl_4^-$ forms an ion- pair ($-N^+(CH_3)_3$-$AuCl_4$) and ligand substitution ($AuBr_4^-$) complexes with the positive head group of CTAB micelles. On the other hand, the reactive species of oxalic acid ($HOOC\text{-}COO^-$) may be assumed to be totally present in the reaction site, i.e., Stern layer as most of the ionic micelle mediated reactions are believed to occur in this region. On the other hand, the $HOOC\text{-}COO^-$ and $AuCl_4^-$ species may be assumed to be totally present in the aqueous pseudo phase due to the electrostatic repulsion between these species and $–OSO_3^-$ of SDS micelles. From the present observations, one can obtain the preliminary role of CTAB and SDS. The key facts are: the reaction proceeds faster in presence of CTAB than in SDS; the final absorbance of AuNPs is higher in SDS and CTAB. In the present case, incorporations and /or associations of reactive species of oxalic acid, $HOOC\text{-}COO^-$ and $AuCl_4^-$ into the micellar palisade- and Stern- layer of CTAB micelles takes place, which in turn, decrease the surface area of the reactants. As a result, reaction proceeds much faster in presence of CTAB. Thus, we may safely conclude that the different nature of spectra (Figs. 3 and 7) is due to the incorporation of $AuCl_4^-$ ions and /or its sol in the Stern layer of CTAB micelles. Coordination of $AuCl_4^-$ anion with $-N^+(CH_3)_3$ captions would increase the electron density of the $AuCl_4^-$ which, in turn, decreases the oxidizing power of the $AuCl_4^-$.

3.4. Mechanism and rate-law

Oxalic acid is relatively strong with $pK_1 = 1.22$ and $pK_2 = 4.28$ ($E_0 = + 0.49$ V for $C_2O_4H_2$ / CO_2 system in acid solution) within the sub-group of weak acids. The pH is an important parameter which governed the nucleation, growth, and active species of the reactants exist in an aqueous solution. Stability

ISSN 2291-6458 (Print), ISSN 2291-6466 (Online)
Year 2013 | Volume 1 | Issue 4 | Page 238-252

of metal nanoparticles depends strongly on the pH of the working reaction mixture and its growth can be stopped by adding the small amounts of minerals acids [29]. In order to establish the reactive species of oxalic acid, pH of the working solution were also measured in presence of different amounts of CTAB and /or oxalic acid. The pH values was found to be nearly constant (pH = 3.2 ± 0.1) with increasing concentrations of CTAB (from 10.0 to 40.0 × 10^{-4} mol dm^{-3}) and [oxalic acid] (from 20.0 to 40.0 × 10^{-4} mol dm^{-3}). Under our experimental conditions, HOOC-COO^- is the major and reactive species of oxalic acid. On the basis of these observations, the Schemes 2 and 3 mechanisms are proposed for the formation of AuNPs.

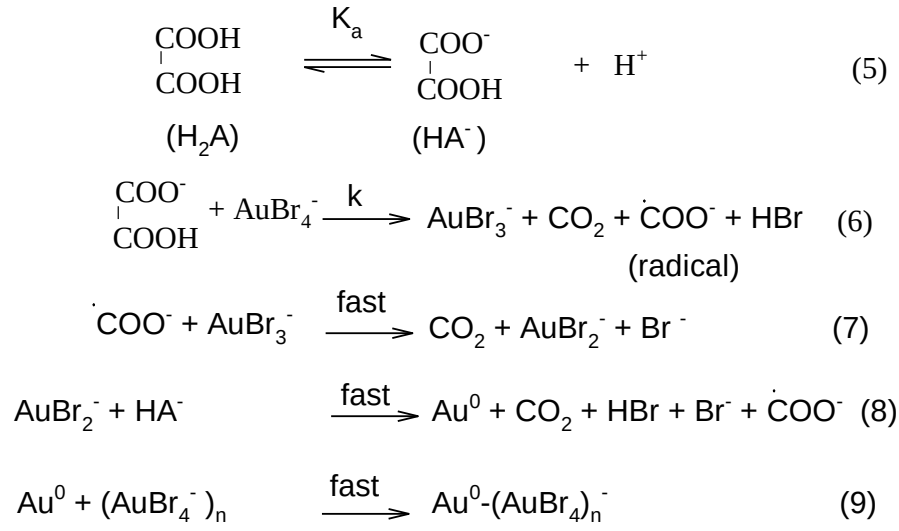

Scheme 2. Reduction of $AuBr_4^-$ by oxalic acid

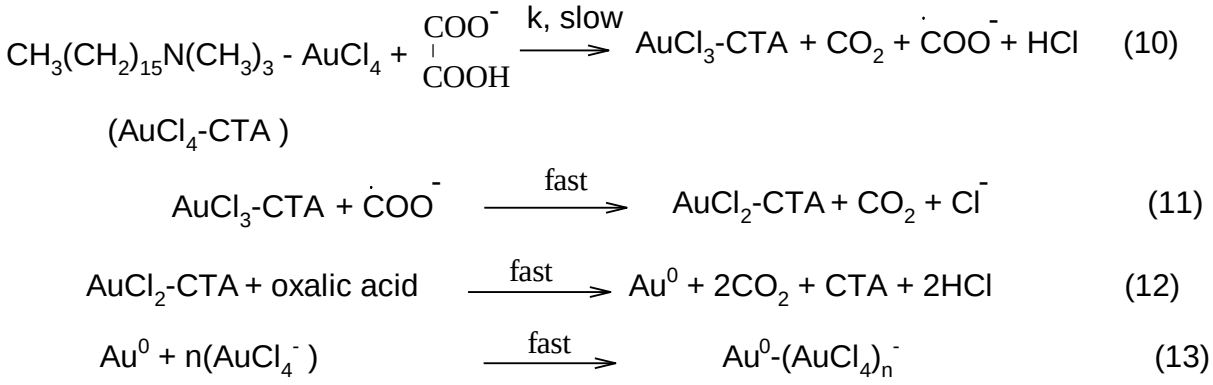

Scheme 3. Reduction of $AuCl_4$-CTA ion-pair complex by oxalic acid

In these schemes, Eq.(6) and (10) are the rate-determining steps (one-electron oxidation-reduction mechanism), leads to the formation of free radical, Au^{3+} and CO_2 as the reaction products. Radical converted into the stable oxidation products, i.e., CO_2 after fast decarboxylation (Eqs. 7 and 11). $AuBr_2$ and $AuCl_2$-CTA species further reacts with another molecule of oxalic acid and ultimately Au^0 is formed after the series of reactions. Eqs. (9) and (13) represents the adsorption of $AuBr_4^-$ and/or $AuCl_4^-$ onto the surfaces of Au^0 . The mechanistic steps (Eqs. 4, 6, and 10) and above observations leads the rate law

ISSN 2291-6458 (Print), ISSN 2291-6466 (Online)
Year 2013 | Volume 1 | Issue 4 | Page 238-252

(Eqs. 14). The rate law or rate equation for a chemical reaction is an equation that links the reaction rate with concentrations of reactants and constant parameters, normally rate coefficients and partial reaction orders.

$$\frac{d[\text{gold sol}]}{dt} = \frac{k\ K_a\ [\text{oxalic acid}]_T\ [\ AuBr_4^-\ \text{or Au-CTA}]}{(K_a + [H^+])} \qquad (14)$$

Eq. (14) explains the first- order dependence of the reaction on [oxalic acid] and [gold species] and rates of AuNPs formation is inversely proportional to the $[H^+]$. The derived rate-equation is in good agreement with the results of Harada *et al*. to the photoreduction of silver perchlorate in aqueous ethanol solution of poly(N-vinyl-2-pyrrolidone) and in water/ sodium bis(2-ethylhexyl) sulfosuccinate/benzene microemulsions [30] and Huang et al. to the spontaneous formation of silver particles in basic 2-propanol [17].

4. CONCLUSION

In summary, we have reported the spectroscopic and visual evidences to the formation of Au(III)-CTAB complexes and its reduction by oxalic acid (preparation of platonic Au-nanoparticles) for the first time. It was found that absorbance and shape of the spectra of Au(III)-CTAB complexes decreases with [CTAB]. TEM results indicate that morphology (nano-chains and nanonetworks-like gold) depends on the ratios of Au(III)-CTAB and oxalic acid concentrations. We also demonstrated that SDS proved very efficient in forming nanoparticles from $HAuCl_4$ in aqueous solutions at room temperature in comparison to CTAB. SDS did not contribute to reduction of $HAuCl_4$. It provides only adsorption, and stabilization functions whereas, CTAB involved in the complexation, ion-pair formation and reduction processes. The preparation route is very mild, and attractive for potential applications regarding the complex formation between gold salt and used stabilizers. The primary investigation shows that the AuIII) complex cannot be formed in presence of SDS.

ACKNOWLEDGMENT

This research work was funded by the Deanship of Scientific Research (DSR), King Abdulaziz Univeristy, Jeddah, under grant number (171/130/1433). The authors, therefore, acknowledge with thanks DSR for technical and financial support.

APPENDIX. Derivation of rate equation

According to Scheme 2

$$\frac{d[\text{gold sol}]}{dt} = k[HA^-]\,[AuBr_4^-] \qquad (I)$$

$$K_a = \frac{[HA^-]\,[H^+]}{[H_2A]}$$

$$[H_2A] = \frac{[HA^-]\,[H^+]}{K_a} \qquad (II)$$

ISSN 2291-6458 (Print), ISSN 2291-6466 (Online)
Year 2013 | Volume 1 | Issue 4 | Page 238-252

The total concentration of oxalic acid is given by

$$[\text{oxalic acid}]_T = [H_2A] + [HA^-]$$

$$= \frac{[HA^-]\,[H^+]}{K_a}$$

$$[HA^-] = \frac{[\text{oxalic acid}]_T\, K_a}{(K_a + [H^+])} \qquad \text{(III)}$$

Substituting the value of $[HA^-]$ in Eq. (I), we get

$$\frac{d[\text{gold sol}]}{dt} = \frac{k\, K_a [\text{oxalic acid}]_T\, [AuBr_4^-]}{(K_a + [H^+])} \qquad \text{(IV)}$$

and for Au-CTA complex

$$\frac{d[\text{gold sol}]}{dt} = \frac{k\, K_a [\text{oxalic acid}]_T\, [\text{Au-CTA}]}{(K_a + [H^+])} \qquad \text{(V)}$$

REFERENCES AND NOTES

[1] (a) Grzelczak, M.; Perez-Juste, J.; Mulvaney, P.; Liz-Marzan, L. M. Shape control in gold nanoparticle synthesis, *Chem. Soc. Rev.* **2008**, *37*, 1783–1791. (b) Perez-Juste, J.; Pastoriza-Santos, I.; Liz-Marzan, L. M.; Mulvaney, P. Gold nanorods: Synthesis characterization and applications, Coordination *Chem. Rev.* **2005**, *249*, 1870–1901. (c) Ji, X.; Song, X.; Li, J.; Bai, Y.; Yang, W.; Peng, X. Size control of gold nanocrystals in citrate reduction: The third role of citrate, *J. Am. Chem. Soc*. **2007**,*129*, 13939-13948. (d) Homan, K. A.; Chen, J.; Schiano, A.; Mohamed, M.; Willets, K. A.; Murugesan, S.; Stevenson, K. J.; Emelianov, S. Silver-polymer composite stars: Synthesis and applications, *Adv. Funct. Mater.* **2011**, *21*, 1673–1680. (e) Xiao, J.; Qi, L. Surfactant-assisted, shape-controlled synthesis of gold nanocrystals, *Nanoscale.* **2011**, *3*, 1383-1396.

[2] (a) Jana, N. R.; Gearheart, L.; Murphy, C. J. Wet chemical synthesis of high aspect ratio cylindrical gold nanorods, *J. Phys. Chem. B.* **2001**, *105*, 4065-4067. (b) Perez-Juste, J.; Liz-Marzan, L. M.; Carnie, S.; Chan, D. Y. C.; Mulvaney, P. Electric-field-directed growth of gold nanorods in aqueous surfactant solutions, *Adv. Funct. Mater.* **2004**, *14*, 571-579. (c) Millstone, J. E.; Park, S.; Shuford, K. L.; Qin, L.; Schatz, G. C.; Mirkin, C. A. Observation of a quadrupole plasmon mode for a colloidal solution of gold nanoprisms, *J. Am. Chem. Soc.* **2005**, *127*, 5312-5313.

[3] (a) Pileni, M.-P. The role of soft colloidal templates in controlling the size and shape of inorganic nanocrystals, *Nature Materials.* **2003**, *2*, 145-150. (b) Jana, N. R.; Gearheart, L.; Murphy, C. J. Seed-mediated growth approach for shape-controlled synthesis of spheroidal and rod-like gold nanoparticles using a surfactant template, *Adv. Mater.* **2001**, *13*, 1389-1393.

[4] Esumi, K.; Matsuhisa, K.; Torigoe, K. Preparation of rod like gold particles by UV irradiation using cationic micelles as a template, *Langmuir.* **1995**, *11*, 3285-3287.

ISSN 2291-6458 (Print), ISSN 2291-6466 (Online)
Year 2013 | Volume 1 | Issue 4 | Page 238-252

[5] Nikoobakht, B.; El-Sayed, M. A. Preparation and growth mechanism of gold nanorods (NRs) using seed-mediated growth method, *Chem. Mater.* **2003**, *15*, 1957-1962.

[6] Sau, T. K.; Murphy, C. J. Room temperature, high-yield synthesis of multiple shapes of gold nanoparticles in aqueous solution, *J. Am. Chem. Soc.* **2004**, *126*, 8648-8649.

[7] Chen, S.; Wang, Z. L.; Ballato, J.; Foulger, S. H.; Carroll, D. L. Monopod, bipod, tripod, and tetrapod gold nanocrystals, *J. Am. Chem. Soc.* **2003**, *125*, 16186-1687.

[8] (a) Miranda, O. R.; Dollahon, N. R.; Ahmadi, T. S. Critical concentrations and role of ascorbic acid (Vitamin C) in the crystallization of gold nanorods within hexadecyltrimethyl ammonium bromide (CTAB)/tetraoctyl ammonium bromide (TOAB) micelles, C*ryst. Growth Des.* **2006**, *6*, 2747-2753. (b) Ma, Y.; Kuang, Z. Jiang, Q.; Xie, Z.; Huang, R.; Zheng, L. Synthesis of trisoctahedral gold nanocrystals with exposed high-index facets by a facile chemical method, *Angew. Chem., Int. E*d., **2008**, *47*, 8901-8904. *(c) Kim, D. Y.; Im, S. H.; Park, O. O.* Synthesis of tetrahexahedral gold nanocrystals with high-index facets, *Cryst. Growth Des. **2010**, 10, 3321-3323.*

[9] (a) Hu, J.; Zhang, Y.; Liu, B.; Liu, J.; Zhou, H.; Xu, Y.; Jiang, Y.; Yang, Z.; Tian, Z.-Q. Synthesis and properties of tadpole-shaped gold nanoparticles, *J. Am. Chem. Soc.* **2004**, *126*, 9470-9471. (b) Joseph, D.; Geckeler, K. E. Surfactant-directed multiple anisotropic gold nanostructures: Synthesis and surface-enhanced Raman scattering, *Langmuir.* **2009**, *25*, 13224-13231. (c) Pallavicini, P.; Chirico, G.; Collini, M.; Dacarro, G.; Dona, A.; Alfonso, L. D; Falqui, A.; Diaz-Fernandez, Y.; Freddi, S.; Garofalo, B.; Genovese, A.; Sironi, L.; Taglietti, A. Synthesis of branched Au nanoparticles with tunable near-infrared LSPR using a zwitterionic surfactant, *Chem. Commun.* **2011**, *47*, 1315-1317.

[10] Lu, X.;Yavuz, M. S.; Tuan, H.-Y.; Korgel, B. A.; Xia, Y. Ultrathin gold nanowires can be obtained by reducing polymeric strands of oleylamine-AuCl complexes formed via aurophilic interaction, *J. Am. Chem. Soc.***2008**, *130*, 8900-89001.

[11] Li, L.; Wang, Z.; Huang, T. ; Xie, J.; Qi, L. Porous gold nanobelts templated by metal-surfactant complex nanobelts, *Langmuir.* **2010**, *26*, 12330-12335.

[12] Turkevitch, J.; Stevenson, P. C.; Hillier, J. Nucleation and growth process in the synthesis of colloidal gold, Discuss. *Faraday Soc.* **1951**, *11*, 55-75.

[13] (a) Chow, M. K.; Zukoski, C. F. Gold sol formation mechanisms role of colloidal stability, *J Colloid Interface Sci.* **1994**, *165*, 97-109. (b) Hanglein, A. Colloidal silver nanoparticles: Photochemical preparation and interaction with O_2, CCl_4, and some metal ions, *Chem Mater.* **1998**, *10*, 444-450. (c) Patakfalvi, R.; Viranyl, Z.; Dekany, I. Kinetics of silver nanoparticle growth in aqueous polymer solutions, *Colloid Polym. Sci.* **2004**, *283*, 299-305.

[14] Ji, X.; Song, X.; Li, J.; Bai, Y.; Yang, W.; Peng, X. Size Control of Gold Nanocrystals in citrate reduction: The third role of citrate, *J Am Chem Soc.* **2007**, *129*, 13939-13948. (e) Polte, J.; Ahner, T. T.; Delissen, F.; Sokolov, S.; Emmerling, F.; Thunemann, A. F.; Kraehnert, R. Mechanism of gold nanoparticle formation in the classical citrate synthesis method derived from coupled in situ XANES and SAXS evaluation, *J. Am. Chem. Soc.* **2010**, *132*, 1296-1301.

[15] Zhang, Q.; Hu, Y.; Guo, S.; Goebl, J.; Yin, Y. Seeded growth of uniform Ag nanoplates with high aspect ratio and widely tunable surface plasmon bands, *Nano Lett.* **2010**, *10*, 5037-5042.

[16] Zhang, Q.; Li, N.; Goeb, J.; Lu, Z.; Yin, Y. A systematic study of the synthesis of silver nanoplates: Is citrate a "Magic" Reagent?, *J. Am. Chem. Soc.* **2011**, *133*, 18931-18939.

[17] Khan, Z.; Singh, T.; Hussain, J. I.; Hashmi, A. A. Au(III)-CTAB reduction by ascorbic acid: preparation and characterization of gold nanoparticles, *Colloids Surfs., B: Biointerfaces.* **2013**, *104*, 11-17.

[18] Huang, Z.-Y.; Mills, G.; Hajek, B. Spontaneous formation of silver particles in basic 2-propanol, *J. Phys. Chem.* **1993**, *97*,11542-11550.

[19] Khan, Z.; Al-Thabaiti, S. A.; Obaid, A. Y.; Khan, Z. A.; Al-Youbi, A. O. Shape-directing role of cetyltrimethylammonium bromide in the preparation of silver Nanoparticles, *J. Colloid Interface Science.* **2012**, *367*, 101-108.

ISSN 2291-6458 (Print), ISSN 2291-6466 (Online)
Year 2013 | Volume 1 | Issue 4 | Page 238-252

[20] Khan, Z.; Hussain, J. I.; Al-Thabaiti, S. A.; Malik, M. A.; Al-Youbi, A. O. Effects of Surfactants on the Morphology of advanced nanomaterials in aqueous solution, *Int. J. Electrochem. Sci.* **2013**, *8*, 204-218.

[21] Khan, Z.; Gupta, D.; Khan, A.A. Kinetics and mechanism of decarboxylation of aspartic acid with ninhydrin, *Int. J. Chem. Kinet.* **1992,** *24*, 481-485.

[22] Torigoe, K.; Esumi, K. Preparation of colloidal gold by photoreduction of tetracyanoaurate(-)-cationic surfactant complexes, *Langmuir.* **1992**, *8*, 59-63.

[23] Elding, L. I.; Groning, A. B. Kinetics, mechanism and equilibria for halide substitution process of chloro bromo complexes of gold(III), *Acta Chem. Sacnd. A.* **1978**, *23*, 867-877.

[24] (a) Nikoobakht, B.; El-Sayed, M.A. Evidence for bilayer assembly of cationic surfactants on the surface of gold nanorods, *Langmuir.* **2001**, *17*, 6368-6374. (b) Gao, J.; Bender, C.M.; Murphy, C.J. Dependence of the gold nanorod aspect ratio on the nature of the directing surfactant in aqueous solution, *Langmuir.* **2003**, *19*, 9065-9070.

[25] (a) Link, S.; El-Sayed, M. A. Spectral properties and relaxation dynamics of surface plasmon electronic oscillations in gold and silver nanodots and nanorods, *J. Phys. Chem. B.* **1999**, *103*, 8410-8426. (b) Link, S.; El-Sayed, M. A. Optical properties and ultrafast dynamics of metallic nanocrystals, *Annu. ReV. Phys. Chem.* **2003**, *54*, 331-366.

[26] Bunton, C. A. The dependence of micellar rate effects upon reaction mechanism, *Ad. Colloid Interface Sci.* **2006**, *123*, 333-343.

[27] Guo, J.-W.; He, X.-M.; Li, J.-J.; Liu, Z.-X.; Pu, W.-H.; Wang, C. US Patent, US20120046482 A1.

[28] (a) Quinten, M.; Schonauer, D.; Kreibig, U. Electronic excitations in many-particle systems: a quantitative analysis, *Z. Phys. D.* **1989**, *12*, *12*521-525. (b) Longenberger, L.; Mills, G. Formation of metal particles in aqueous solutions by reactions of metal complexes with polymers, *J. Phys. Chem.* **1995**, *99*, 475-852.

[29] Rodriguez-Fernandez, J.; Perez-Juste, J.; Mulvaney, P.; Liz-Marzan, L.M. Spatially-directed oxidation of gold nanoparticles by Au(III)-CTAB complexes, *J. Phys. Chem. B.* **2005**, *109*, 14257-14261.

[30] Ershov, B. G.; Janata, E.; Henglein, A. Silver atoms and clusters in aqueous solution: absorption spectra, and the particle growth in the absence of stabilizing Ag^+ ions, *J. Phys. Chem.* **1993**, *97*, 4589-4594.

[31] Harada, M.; Saijo, K.; Sakamoto, N.; Ito, K. Characterization of water/AOT/benzene microemulsions during photoreduction to produce silver particles, *J. Colloid Interface Sci.* **2010**, *343*, 423-432.

The authors declare no conflict of interest